

Integral equation study of soft-repulsive dimeric fluids

Gianmarco Munaò^{1,*}, Franz Saija^{2,†}

¹*Dipartimento di Scienze Matematiche e Informatiche,
Scienze Fisiche e Scienze della Terra,
Università degli Studi di Messina,
Viale F. Stagno d'Alcontres 31, 98166 Messina, Italy.*
and

²*CNR-IPCF, Viale F. Stagno d'Alcontres 37, 98158 Messina, Italy.**

We study fluid structure and water-like anomalies of a system constituted by dimeric particles interacting via a purely repulsive core-softened potential by means of integral equation theories. In our model, dimers interact through a repulsive pair potential of inverse-power form with a softened repulsion strength. By employing the Ornstein-Zernike approach and the reference interaction site model (RISM) theory, we study the behavior of water-like anomalies upon progressively increasing the elongation λ of the dimers from the monomeric case ($\lambda = 0$) to the tangent configuration ($\lambda = 1$). For each value of the elongation we consider two different values of the interaction potential, corresponding to one and two length scales, with the aim to provide a comprehensive description of the possible fluid scenarios of this model. Our theoretical results are systematically compared with already existing or newly generated Monte Carlo data: we find that theories and simulations agree in providing the picture of a fluid exhibiting density and structural anomalies for low values of λ and for both the two values of the interaction potential. Integral equation theories give accurate predictions for pressure and radial distribution functions, whereas the temperatures where anomalies occur are underestimated. Upon increasing the elongation, the RISM theory still predicts the existence of anomalies; the latter are no longer observed in simulations, since their development is likely precluded by the onset of crystallization. We discuss our results in terms of the reliability of integral equation theories in predicting the existence of water-like anomalies in core-softened fluids.

I. INTRODUCTION

The reference interaction site model (RISM) theory, formulated in the early 70's by Chandler and Andersen [1, 2], is still one of the most adopted structural theories of molecular fluids. In the RISM approach, developed as a generalization of the Ornstein-Zernike theory of atomic fluids [3], the molecules are represented as a collection of spherical interaction sites, rigidly connected so to reproduce a given molecular geometry [4]. Originally the theory was developed to deal only with hard-sphere fluids [5] or with simple Lennard-Jones systems [6]. Later on, the RISM framework has been extended to take into account more realistic representations of complex fluids, including water, methanol and other compounds (see Refs [7–11] and a general review in Ref. [12]). More recently, the RISM approach (along with its extensions and generalizations) has been adopted for predicting structure, thermodynamic and phase equilibria of a large variety of systems, including dumbbell fluids [13–15], colloids [16, 17], proteins [18, 19], surfactants [20, 21] and water solutions [22, 23]. In the last years further refinements of the original RISM theory have made possible the development of more complex approaches, as for instance the three dimensional reference interaction site model theory [24–26] and the multi-center molecular Ornstein-Zernike equation [27].

The structure and the phase behavior of complex fluids is of great interest in the field of liquid and soft matter physics. This is especially due to the peculiar thermodynamic and structural properties exhibited by some of these fluids, named anomalous liquids. Water is the most known example of such fluids; its peculiar behaviors, including re-entrant melting and density anomalies, have been largely investigated both from experimental [28–32] and theoretical [33–38] points of view. The existence of these anomalies has been traditionally related to the possibility to develop a network between water molecules through hydrogen bonds.

Within this framework a modeling approach, which is arousing an increasing interest in the last years, is based on spherically symmetric core-softened (CS) potentials: according to this approach, formulated by Hemmer and Stell in 1970 [39], in these potentials the hard-core interactions turn to be softened and an attractive tail is set. A large variety of studies has been carried out to investigate the peculiar physical properties of these potentials, with a particular focus on liquid-liquid phase transition [40–44] and water-like anomalies [45–52]. In this context, the RISM theory has been successfully adopted, along with the Mode-Coupling theory, to study the pressure dependence of the diffusion coefficient for acetonitrile and methanol in water [53] and to analyze the phase behavior of a number of CS molecular models [54, 55].

In this work we investigate structure and thermodynamics of a simple model for a dimeric fluid interacting via a modified inverse-power potential (MIP) [56, 57] by means of RISM theory and Monte Carlo (MC) simulations. In a previous study [58] we have shown that a sys-

* Corresponding author: gmunao@unime.it

† franz.saija@cnr.it

tem of dimeric particles interacting through MIP displays typical water-like anomalies, like a temperature of maximum density (TMD) and a non-monotonic behavior of the pair translational entropy. Also, we have investigated how the existence of such anomalies depends on the elongation of the dimers and on the interaction potential parameters. In particular, upon increasing the repulsion softening, it has been possible to study how the fluid structure is changed when going from one-scale behavior typical of Lennard-Jones fluids to a two-scale behavior characterizing the CS systems.

Here we extensively employ the RISM framework for calculating structural and thermodynamic properties of the dimer fluid interacting via MIP, in the whole range of elongations and for two different values of the repulsion softening. For this purpose we adopt and compare hypernetted chain (HNC) [3] and Kovalenko-Hirata (KH) [59, 60] approximation closures and various routes from the structure to thermodynamics. Where possible, theoretical results are assessed against previous [58] or newly generated MC simulations performed in the canonical ensemble. This work has been carried out with the aim to investigate the anomalous behaviors of the dimer fluid in a wide range of parameters; also, to the best of our knowledge, this study constitutes the first application of the RISM approach to investigate density and structural anomalies in a molecular fluid interacting via a CS potential.

The paper is organized as follows: in the next section we provide details of the model, the RISM theory and the simulation approach. Results are presented and discussed in the third section and conclusions follow in the last section.

II. MODEL, THEORY AND SIMULATIONS

A schematic representation of some models investigated in this work is reported in Fig. 1: in a first instance we consider the monomeric case, corresponding to two totally overlapped spheres. Then, the distance between the centres of the spheres is progressively increased. By indicating with λ such a distance, our scheme is equivalent to move from $\lambda = 0$ (total overlap) to $\lambda = 1$ (tangent dimer). We set a site-site interaction potential written as [56]:

$$U(r) = \epsilon(\sigma/r)^{n(r)} \quad (1)$$

where r is the distance between spheres belonging to different dimers, ϵ and σ are the units of energy and length, respectively, and

$$n(r) = n_0 \{1 - \alpha \exp[-b(1 - r/\sigma)^2]\}. \quad (2)$$

In Eq. (2) α is a real number whose value is in the range $[0, 1]$, whereas b and n_0 are positive integer numbers. In this work we make use of the reduced units by defining reduced temperature, density and pressure as, respectively,

$T^* \equiv k_B T/\epsilon$, $\rho^* \equiv \rho\sigma^3$ and $P^* \equiv P\sigma^3/\epsilon$, where k_B is the Boltzmann constant.

In Eqs. 1-2 the repulsion softening is controlled by the parameter α , whereas b set the width of the interval where $n(r)$ is smaller than n_0 . In all calculations the values of $b = 5$ and $n_0 = 12$ are kept fixed; as for the values of α , we consider two different cases, namely $\alpha = 0.6$ and $\alpha = 0.8$. In Fig. 2 we report the behavior of $U(r)$ for these two values: as observed, for $\alpha = 0.6$ the potential decays by following an inverse-power law, whereas for $\alpha = 0.8$ an inflection point with a corresponding change of the concavity is found. Under these conditions, $U(r)$ exhibits two different length scales, as typical for CS systems. We remark that our interparticle potential is purely repulsive, hence the relative phase diagram will not exhibit a gas-liquid phase transition, even if in principle a metastable liquid-liquid phase transition could be present [61].

In order to investigate the fluid structure of the monomeric model (i.e. $\lambda = 0$) we have employed the Ornstein-Zernike equation for simple fluids, [3] expressed in the k -space (for an homogeneous and isotropic fluid) as:

$$\mathbf{h}(k) = \mathbf{c}(k) + \rho \mathbf{c}(k) \mathbf{h}(k) \quad (3)$$

where $\mathbf{h}(k)$ and $\mathbf{c}(k)$ are the Fourier transforms of the total and direct correlation functions $h(r)$ and $c(r)$ and ρ is the density of the system. In order to solve Eq. (3), we have adopted in this work the hypernetted chain (HNC) expression [3]:

$$c(r) = \exp[-\beta U(r) + \gamma(r)] - \gamma(r) - 1 \quad (4)$$

where $\beta = 1/T^*$ and $\gamma(r) = h(r) - c(r)$. In parallel to HNC, we have employed its partially linearized form, developed by Kovalenko and Hirata (KH) [59, 60] that amounts to set:

$$c(r) = \begin{cases} \text{HNC} & \text{if } g(r) \leq 1 \\ \text{MSA} & \text{if } g(r) > 1 \end{cases}, \quad (5)$$

with MSA (mean spherical approximation) corresponding to assume [3]:

$$\begin{cases} g(r) = 0 & \text{if } r \leq \sigma \\ c(r) = -\beta U(r) & \text{if } r > \sigma \end{cases}, \quad (6)$$

where $g(r) = h(r) + 1$.

For $\lambda > 0$, the Ornstein-Zernike equation can not be implemented and a molecular generalization is required. In the present work we apply the RISM framework [2] where the pair structure of a fluid composed by identical two-site molecules is characterized by a set of four site-site intermolecular pair correlation functions $h_{ij}(r)$ where $(i, j) = (1, 2)$. The $h_{ij}(r)$ are related to a set of intermolecular direct correlation functions $c_{ij}(r)$ by a matrix generalization of Eq. (3), written in the k -space as:

$$\mathbf{H}(k) = \mathbf{W}(k) \mathbf{C}(k) \mathbf{W}(k) + \rho \mathbf{W}(k) \mathbf{C}(k) \mathbf{H}(k) \quad (7)$$



FIG. 1. Cartoons of some models investigated in this work: starting from 0 (left), λ is progressively increased up to 1 (right). Intermediate cases, as for instance $\lambda = 0.6$ (center), have been also investigated.

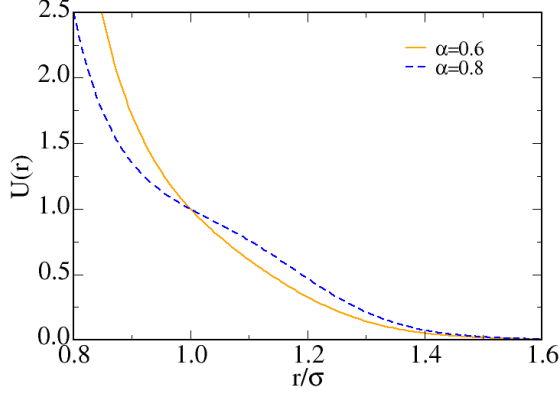


FIG. 2. Site-site intermolecular potential $U(r)$ for $\alpha = 0.6$ (full line) and for $\alpha = 0.8$ (dashed line).

where $\mathbf{H} \equiv [h_{ij}(k)]$, $\mathbf{C} \equiv [c_{ij}(k)]$, and $\mathbf{W} \equiv [w_{ij}(k)]$ are 2×2 symmetric matrices; the elements $w_{ij}(k)$ are the Fourier transforms of the intramolecular correlation functions, written explicitly as:

$$w_{ij}(k) = \frac{\sin[kL_{ij}]}{kL_{ij}}, \quad (8)$$

where the bond length L_{ij} is given either by $L_{ij} = \sigma$, if $i \neq j$, or by $L_{ij} = 0$, otherwise. In analogy with the monomeric case, we have coupled Eq. (7) with HNC and KH approximations, generalized for molecular fluids.

In order to calculate thermodynamic properties of the monomeric fluid, we have implemented different routes from structure to thermodynamics; specifically, we have adopted and compared virial and compressibility equations of state [3, 62] both in HNC and KH approaches. According to the first route, pressure can be obtained through the standard formula [3]:

$$\frac{\beta P}{\rho} = 1 - \frac{2}{3}\pi\beta\rho \int_0^\infty U'(r)g(r)r^3 dr \quad (9)$$

while in the compressibility route scheme we have [62]:

$$\beta P = \int_0^\rho d\rho' [S(k=0)]^{-1} \quad (10)$$

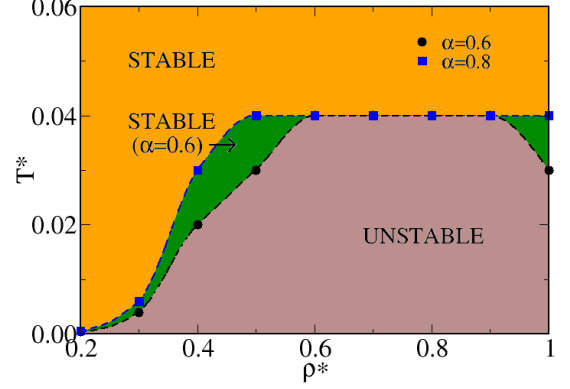


FIG. 3. Stability regions of the HNC algorithm for $\lambda = 0$. In the orange area the numerical convergence is achieved both for $\alpha = 0.6$ and for $\alpha = 0.8$; in the green zone, the convergence is ensured for $\alpha = 0.6$ only, whereas in the brown area the HNC fails to get the convergence regardless of the value of α .

where $[S(k=0)]$ is the $k \rightarrow 0$ limit of the structure factor $S(k)$. For molecular fluids, a direct application of Eq. (9) is not straightforward, since the knowledge of site-site $g_{ij}(r)$ is not enough for the calculation of the pressure. Hence, for $\lambda > 0$ we have implemented a closed formula derived in the context of HNC approximation [63, 64] and generalized for the KH closure [60] as:

$$\begin{aligned} \frac{\beta P}{\rho} = & 1 + \frac{\rho}{2} \sum_{ij} \int d\mathbf{r} \left[\frac{1}{2} h_{ij}^2(r) \Theta(-h_{ij}(r)) - c_{ij}(r) \right] \\ & + \frac{1}{2(2\pi)^3} \int d\mathbf{k} \{ \rho^{-1} \ln \det [\mathbf{I} - \rho \mathbf{W}(k) \mathbf{C}(k)] \\ & - \text{Tr} [\mathbf{W}(k) \mathbf{C}(k)] [\mathbf{I} - \rho \mathbf{W}(k) \mathbf{C}(k)]^{-1} \} \quad (11) \end{aligned}$$

where Θ is the Heaviside step function. As for the compressibility route (see Eq. (10)) its validity is guaranteed in a molecular context also.

We have implemented the numerical solution of both Ornstein-Zernike and RISM schemes by means of a standard iterative Picard algorithm, on a grid of 8192 points with a mesh $\Delta r = 0.005\sigma$. To improve the convergence of the Picard algorithm we have adopted the strategy of mixing old and new $\gamma(r)$ functions with a mixing param-

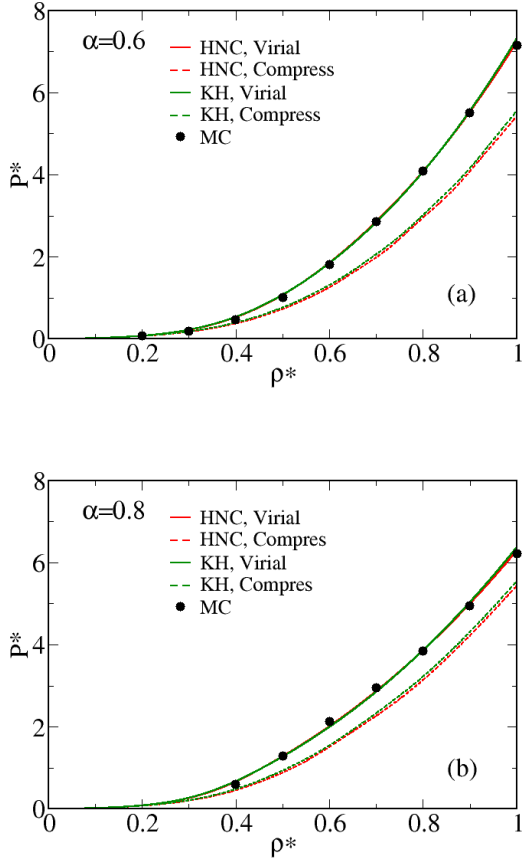


FIG. 4. HNC (red lines), KH (green lines) and MC (symbols) pressures for $\lambda = 0$, $T^* = 0.10$ and $\alpha = 0.6$ (a) and $\alpha = 0.8$ (b). Virial and compressibility routes are indicated by full lines and dashed lines, respectively.

eter of 0.9. This choice allows for an optimization of the convergence procedure for a wide range of temperatures and densities.

Theoretical predictions have been compared with Monte Carlo (MC) simulations performed in the canonical ensemble. We have considered a system composed by 864 dimers in a cubic box with periodic boundary conditions. For any state point we have first performed 2×10^5 steps in order to equilibrate the system, then computing statistical averages on the same number of following steps. For the lowest temperatures investigated, we have employed up to 5×10^5 steps for the equilibration stage; then, an equal number of steps has been generated in the production stage.

III. RESULTS

We have first considered the case $\lambda = 0$. As a preliminary check, we have identified the regions, in the

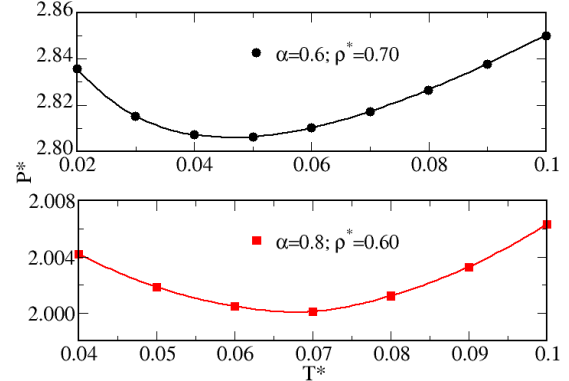


FIG. 5. Pressures versus temperatures for the monomeric case for $\alpha = 0.6$ and $\rho^* = 0.70$ (top) and for $\alpha = 0.8$ and $\rho^* = 0.60$ (bottom), resulting from the HNC virial route.

temperature-density plane, where the HNC numerical algorithm is able to achieve the convergence. Such regions are reported in Fig. 3: the algorithm properly works at all densities for $T^* \geq 0.04$. At lower temperatures, the numerical procedure encounters more and more difficulties to get the fully convergence, until it ceases to work; for $\alpha = 0.8$ this breakdown is observed at temperatures slightly higher than for $\alpha = 0.6$. Conversely, we have verified that the KH closure does not show any convergence problems for $T^* \geq 0.02$ in the whole range of densities and for both $\alpha = 0.6$ and $\alpha = 0.8$. This circumstance allows for the implementation of the KH closure even at low temperatures where HNC is not able to provide predictions.

Simulation and theoretical pressures for $\alpha = 0.6$ and $\alpha = 0.8$ at $T^* = 0.10$ are reported in panels (a) and (b) of Fig. 4, respectively. Ornstein-Zernike predictions have been obtained by following the virial equation (see Eq. (9)) and the compressibility route (see Eq. (10)). Both HNC and KH show a quantitative agreement with the MC data if the virial route is implemented; conversely, the compressibility route systematically underestimates simulation results in the whole density range. Moreover, at this temperature no remarkable differences between HNC and KH are observed. We have also verified that simulation data for internal energy per particle E/N , not shown here, are accurately reproduced by both theories, with only a slight overestimation at intermediate densities.

Upon lowering T^* we document an unusual expansion of the system, with the density progressively increasing until it reaches a maximum and then decreasing. Such a scenario points out to the presence of a temperature of maximum density (TMD), whose value strongly depends on the particular pressure considered. As a consequence, if we look at the behavior of the pressure as a function

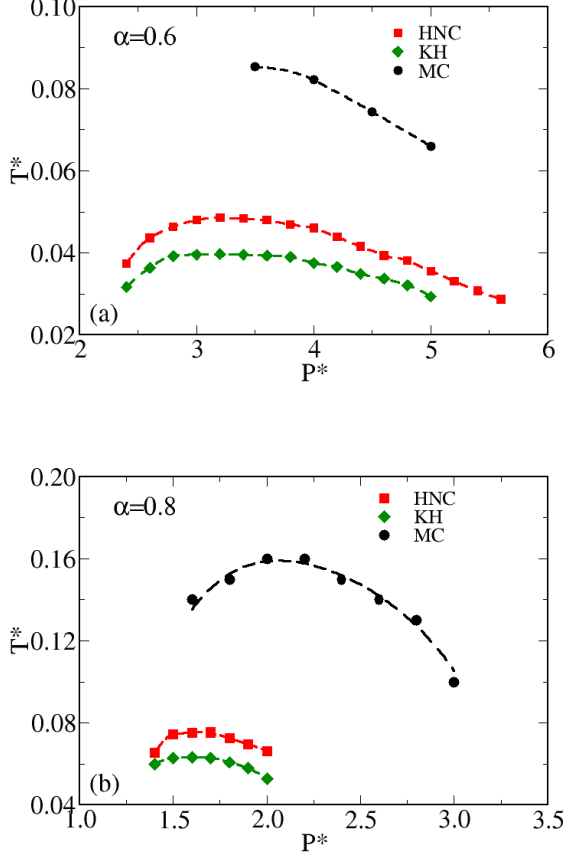


FIG. 6. Loci of TMD points for $\lambda = 0$ with $\alpha = 0.6$ (a) and $\alpha = 0.8$ (b) resulting from HNC, KH and MC. Theoretical predictions have been obtained by the virial route. Lines are guides for the eye.

of the temperature, a minimum is observed at a specific value of the density. Such a minimum is reported in Fig. 5 in the context of HNC virial like for both $\alpha = 0.6$ and $\alpha = 0.8$ at different densities: we observe that for $\alpha = 0.6$ the minimum is located at lower temperatures and higher pressures. This is consistent with the fact that for $\alpha = 0.6$ the TMD is very close to the liquid-solid transition [57].

The specific values attained by the TMD define the density anomaly region in the temperature-pressure plane. Such regions are reported in Fig. 6, where theoretical results have been obtained by employing the virial route only; we have checked that at low temperatures and high densities the HNC compressibility route can hardly be implemented, since the integration of $[S(k=0)]^{-1}$ shows typical oscillations [54] that affect the behavior of the resulting TMD curves, not shown here. In Fig. 6 we note that, despite the quantitative agreement between pressures obtained from MC simulations and from the virial route shown in Fig. 4, the loci of TMD points are

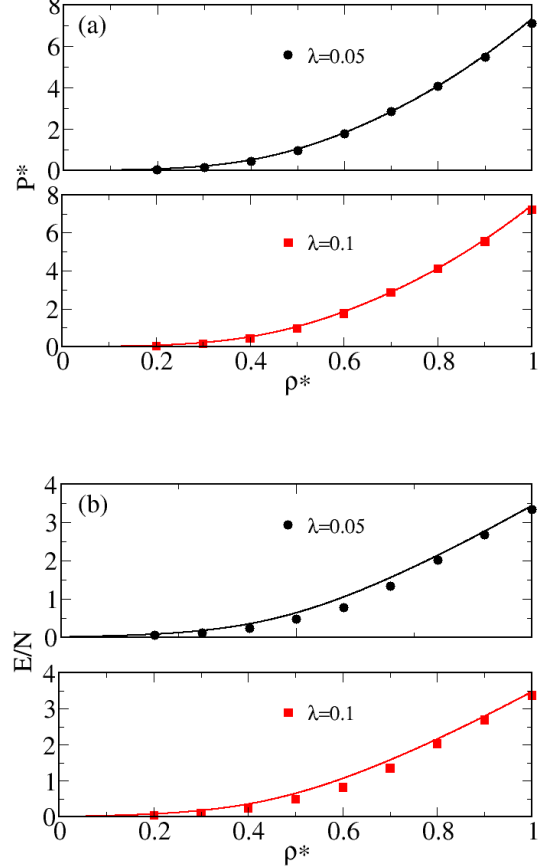


FIG. 7. Pressure (a) and average internal energy per particle (b) for $\alpha = 0.6$, $T^* = 0.075$ and $\lambda = 0.05$ and 0.1 , obtained from KH (lines) and MC (symbols).

underestimated by both KH and HNC, with the latter slightly more predictive. This outcome can be explained by considering that, since the TMD is strongly dependent on the pressure, a tiny difference between the pressure values may give rise to a remarkable difference between the TMD's. It is worth to compare our results with previous integral equations studies of anomalies in simple fluids [65, 66]. In such studies the anomalies have not been observed in the HNC framework, but only in the more refined context of thermodynamically consistent closures, like the Rogers-Young. However, the intermolecular potentials adopted in those studies included also attractive contributions and it is known that the HNC closure hardly deals with attractive potentials in proximity of phase transitions. Hence we desume that HNC is able to detect the presence of fluid anomalies of the MIP potential because the latter does not contain attractive contributions and the anomalous region is located inside the convergence region of the algorithm.

Upon increasing λ , the Ornstein-Zernike approach must be replaced by the RISM framework. We have

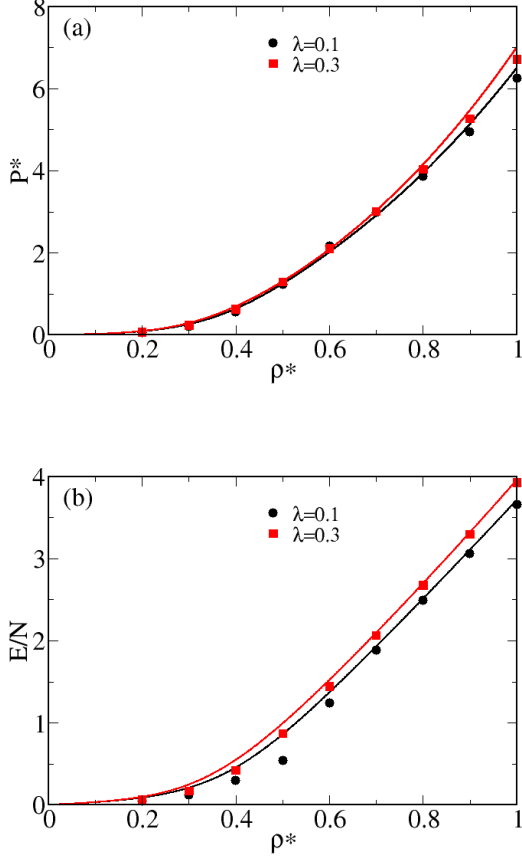


FIG. 8. Pressure (a) and average internal energy per particle (b) for $\alpha = 0.8$, $T^* = 0.075$ and $\lambda = 0.1$ and 0.3 , obtained from KH (lines) and MC (symbols).

verified that the HNC scheme fails to achieve the convergence at low temperatures for $\lambda < 0.2$; such a circumstance precludes the possibility to implement this closure to investigate structural and thermodynamic anomalies for low values of λ . Henceforth we shall make use of the KH closure only, that does not experience such problems and properly works in the whole range of λ values. Also, following the prescription adopted in Ref. [58] and previously suggested by de Oliveira and coworkers [50], pressure and temperature shall be rescaled by a factor 4, in order to ensure a proper comparison with the monomeric case where the effective interparticle interaction is four times weaker.

In Fig. 7 we compare KH and MC results for pressure (a) and internal energy per particle (b) for $\alpha = 0.6$, $T^* = 0.075$ and $\lambda = 0.05$ and 0.1 . Theoretical predictions for the pressure have been obtained by implementing the KH closed formula [60] reported in Eq. (11). As already observed for the monomeric case, pressure is still quantitatively reproduced by the theory both for $\lambda = 0.05$ and for $\lambda = 0.1$. Theoretical predictions for the internal en-

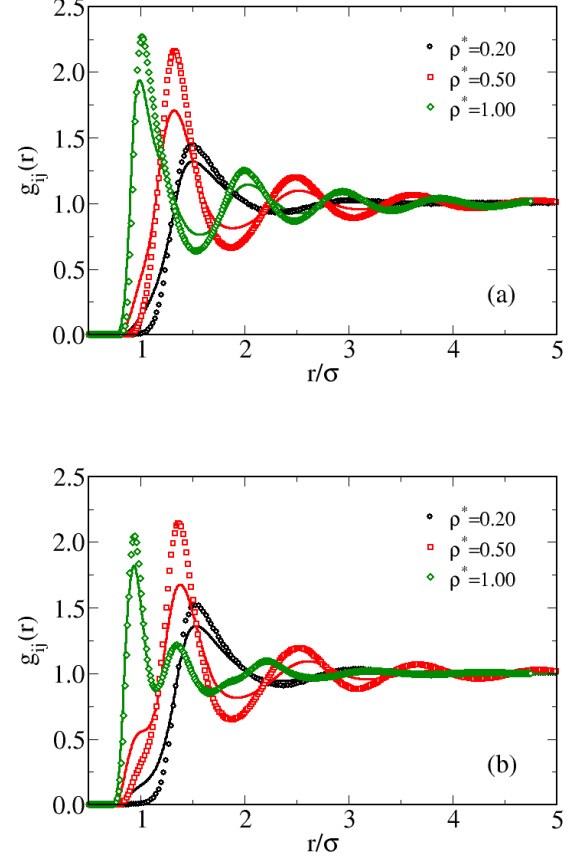


FIG. 9. Site-site $g_{ij}(r)$ for $\alpha = 0.6$ and $\lambda = 0.05$ (a) and for $\alpha = 0.8$ and $\lambda = 0.1$ (b) at $T^* = 0.15$ and various densities obtained from KH (lines) and MC (symbols).

ergy appear less accurate, with an overestimation visible at intermediate densities. Upon increasing α to 0.8 , we find a similar scenario: in Fig. 8 we report simulation and theoretical results for pressure (a) and internal energy per particle (b) for $\alpha = 0.8$, $T^* = 0.075$ and $\lambda = 0.1$ and 0.3 . The theory accurately reproduces simulation results for pressure, but for high densities ($\rho^* > 0.8$) where KH slightly overestimates MC data. The agreement worsens for the internal energy, in particular at intermediate densities as observed for $\alpha = 0.6$.

The local structure of the dimeric fluid is investigated in Fig. 9 where we report KH and MC results for the site-site radial distribution function $g_{ij}(r)$ for $\alpha = 0.6$ and $\lambda = 0.05$ (a) and for $\alpha = 0.8$ and $\lambda = 0.1$ (b) at $T^* = 0.15$ and various densities. The agreement between theory and simulations appears reasonably good in both cases: for $\alpha = 0.6$ the one-scale behavior of the intermolecular potential (see Fig. 2) is clearly visible in the $g_{ij}(r)$. Indeed, upon increasing the density, the first peak is progressively shifted towards lower and lower values of r/σ , as expected for a core-softened fluid subjected to a

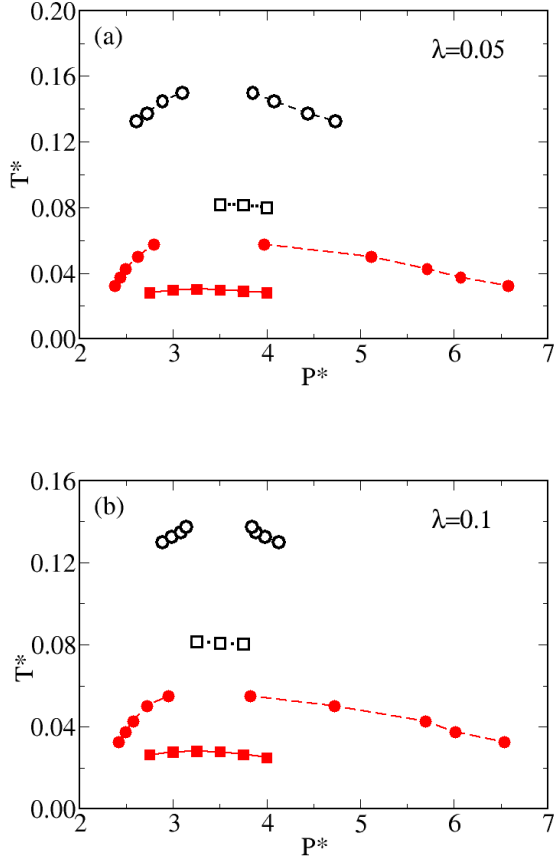


FIG. 10. Loci of structural (circles) and density (squares) anomalies in the pressure-temperature plane for $\alpha = 0.6$ and increasing λ obtained from KH (full symbols) and MC (open symbols). Lines are guides for the eye.

compression. KH closely follows the simulation path, becoming more predictive at high density ($\rho^* = 1.0$). For $\alpha = 0.8$ (b) the behavior of $g_{ij}(r)$ appears quite different; now, a second close-contact peak is found upon increasing the density. Such a peak becomes dominant at $\rho^* = 1.0$ where the system is strongly compressed. This behavior is typical of a fluid exhibiting two length scales in the interaction potential and is observed both in KH and MC $g_{ij}(r)$, with the theory anticipating the onset of the second peak, already visible for $\rho^* = 0.50$.

We now tackle the issue to investigate the behavior of density and structural anomalies as a function of λ for $\alpha = 0.6$ and for $\alpha = 0.8$. As previously discussed, the density anomaly region in the temperature-pressure plane is defined by the values attained by the TMD. The structural anomaly is instead characterized by the unusual behavior of the pair translational entropy S_2 , defined as [67]:

$$S_2/k_B = -\frac{1}{2}\rho \int d\mathbf{r} [g_{cm}(r) \ln g_{cm}(r) - g_{cm}(r) + 1] \quad (12)$$

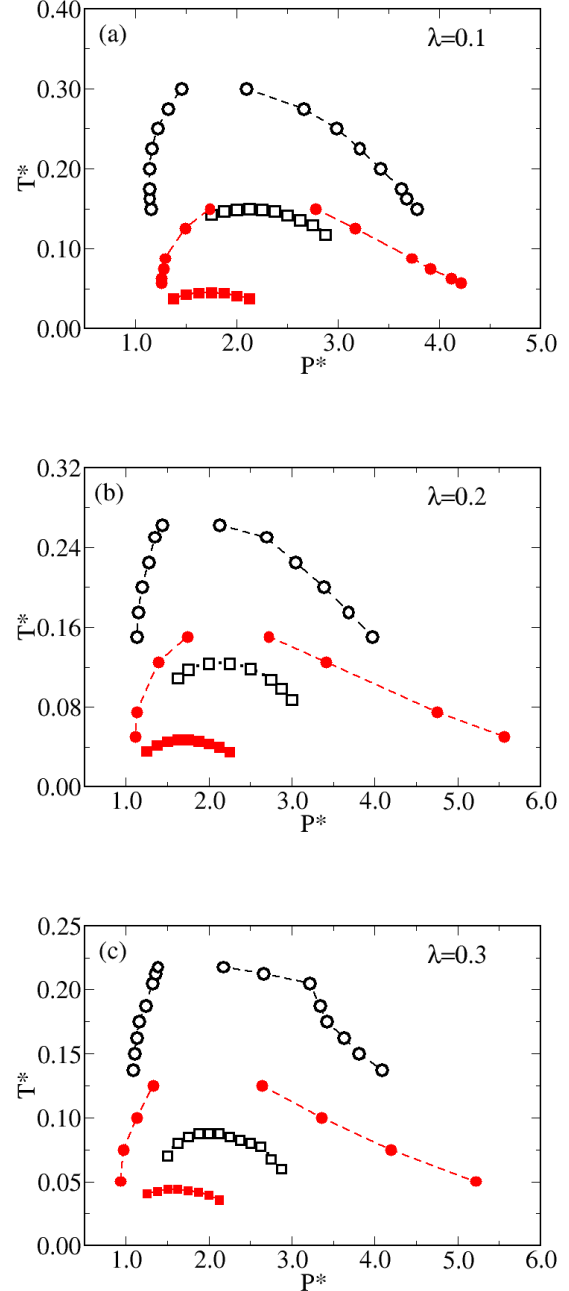


FIG. 11. Loci of structural (circles) and density (squares) anomalies in the pressure-temperature plane for $\alpha = 0.8$ and increasing λ obtained from KH (full symbols) and MC (open symbols). Lines are guides for the eye.

where $g_{cm}(r)$ is the pair distribution function between the centers of mass of two dimers. This quantity is not to be taken as a quantitative measure of the pair entropy of the dimer because the rotational contribution is not considered by Eq. (12). In fact, the orientational term depends on the angles that are needed to specify the relative ori-

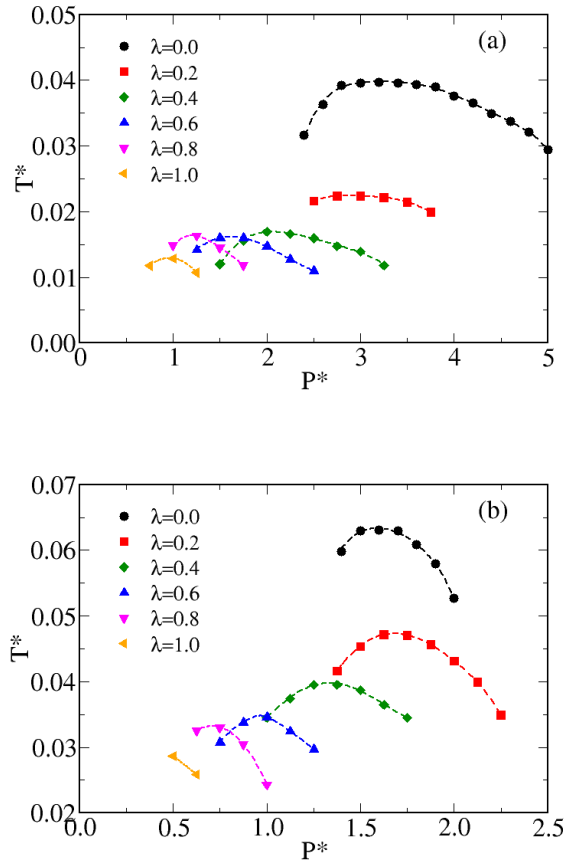


FIG. 12. Loci of TMD points at several values of λ for $\alpha = 0.6$ (a) and $\alpha = 0.8$ (b) obtained from KH. Lines are guides for the eye.

entation. The correlation between the translational and orientational contributions of the pair entropy turns out to be a sensitive indicator of structurally resolved ordering process occurring in molecular liquids [68–72] and it will be subject of a subsequent study [73].

In a simple fluid, $-S_2$ monotonically increases with the density at fixed temperature; conversely, this function shows the presence of a maximum and a minimum for systems interacting through CS potentials [74, 75]. Eq. (12) implies that in principle is not possible to calculate S_2 within the RISM framework, since $g_{cm}(r)$ is not available. Actually, it is possible to introduce non interacting auxiliary sites at the geometric centre of a dimer, with the aim to obtain the pair distribution function between the centers of mass of two dimers. However, it has been already observed [76] that the site-site radial distribution functions show a dependence on these auxiliary sites. Hence, to avoid the introduction of spurious effects on $g_{ij}(r)$, we do not make use of this prescription. Also, we have verified that, for $\lambda \leq 0.3$ the differences between $g_{cm}(r)$ and $g_{ij}(r)$ are not very significant and an (approx-

imate) theoretical calculation of S_2 by putting $g_{ij}(r)$ in Eq. (12) is possible.

The behavior of density and structural anomalies for $\alpha = 0.6$ as functions of λ is reported in Fig. 10. The theory qualitatively follows simulations in predicting the existence of density and structural anomaly regions, even if they are both underestimated, as observed for the locus of TMD points for $\lambda = 0$ (see Fig. 6). In this context, in comparison with our previous simulation study on the MIP dimer fluid [58] we have verified through more refined calculations that the density anomaly survives till to $\lambda = 0.1$.

Density and structural anomalies for $\alpha = 0.8$ are investigated in Fig. 11. As observed for $\alpha = 0.6$, the theory correctly predicts the existence of both of them, underestimating the temperatures where they occur. Interestingly the agreement between MC and KH for the predictions of the TMD progressively improves upon increasing λ . This finding suggests that the theory works better for not too low values of the elongation, where the closeness of the two interaction sites can affects the accuracy of predictions.

KH predictions for the TMD in the whole range of λ values are collectively reported in Fig 12: for $\alpha = 0.6$ (a) we observe a progressive shift of the density anomaly regions towards very low temperatures, with a “saturation” for $\lambda \geq 0.4$. At the same time, pressure attains progressively lower values. A similar scenario holds for $\alpha = 0.8$ (b), but in this case the saturation effect is not observed and the density anomaly region moves towards lower and lower values of T^* . In comparison with simulations, the theory predicts the existence of the TMD for all values of $0 \leq \lambda \leq 1$ for both $\alpha = 0.6$ and $\alpha = 0.8$. On the other hand, simulations predict the existence of the TMD only if $\lambda \leq 0.1$ for $\alpha = 0.6$ and $\lambda \leq 0.3$ for $\alpha = 0.8$. At higher values of λ the development of the density anomaly is likely prevented by the onset of solid phases. However, according to KH predictions, the system persists in a fluid phase down to very low temperatures and hence the development of the TMD is not hampered by a crystallization. This observation can be checked by looking at the behavior of the molecular structure factor $S(k)$ that, for a biatomic molecule, is equivalent to the structure factor between the centers of mass of two dimers. According to the qualitative criterion developed by Hansen and Verlet for the Lennard-Jones potential [77], a fluid system approaches a solid phase when the height of the first peak of the $S(k)$ exceed 2.85. A similar criterion is expected to roughly hold even if a CS potential is adopted. In Fig. 13 we compare MC and KH $S(k)$ obtained for $\lambda = 0.2$, $\alpha = 0.8$ and $T^* = 0.625$: simulation data show a progressive increase of the first peak of the $S(k)$ until it overcomes 3 for densities between 0.40 and 0.60 and the system becomes solid-like. For density higher than 0.60, the first peak decreases and the system becomes fluid again. According to the KH predictions, the increase of the peak is equally observed but it never becomes greater than 3. Rather, it approaches a maximum at 2.5 and then

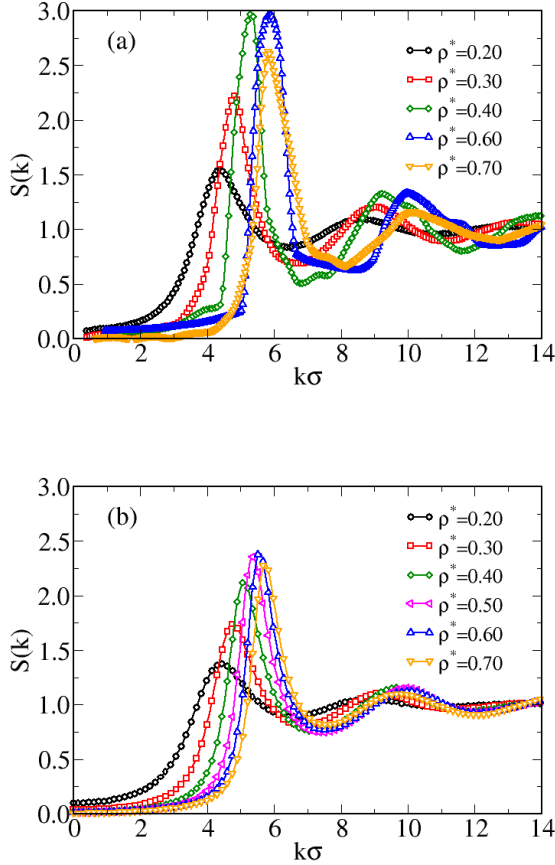


FIG. 13. Structure factors between the centres of mass of two dimers obtained from MC simulations (a) and from KH (b) for $\lambda = 0.2$, $\alpha = 0.8$ and $T^* = 0.0625$.

decreases.

Finally, we have calculated the residual multiparticle entropy ΔS defined as:

$$\Delta S = S_{ex}/N - S_2 \quad (13)$$

with

$$S_{ex}/N = (E/N - A_{ex}/N)/T^* \quad (14)$$

where A_{ex}/N is the excess free energy per particle and S_{ex}/N is the excess entropy per particle. According to the criterion developed by Giaquinta and Giunta [78] ΔS vanishes whenever a fluid system approaches the solidification. It has been shown that the validity of this criterion holds for softly repulsive fluids also [79]. In Fig. 14 we report the residual multiparticle entropy obtained from MC and KH for $\lambda = 0.2$, $\alpha = 0.8$ and $T^* = 0.0625$. Simulation data indicate that ΔS crosses the zero line for $0.4 < \rho^* < 0.6$, whereas KH theory never predicts that ΔS vanishes. Such a result agrees with the behavior of $S(k)$ reported in Fig. 13. The emerging picture confirms

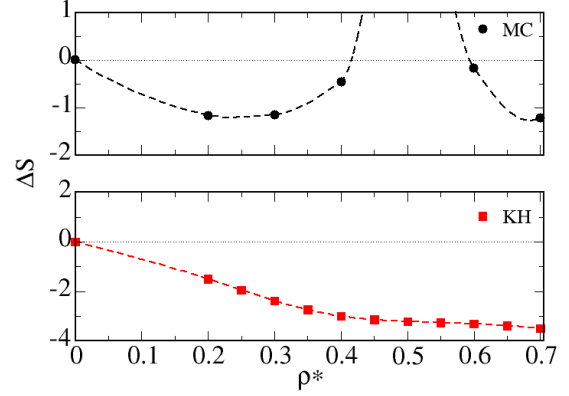


FIG. 14. Residual multiparticle entropy ΔS from MC simulations (circles) and KH (squares) for $\lambda = 0.2$, $\alpha = 0.8$ and $T^* = 0.0625$. Dashed lines are guides for the eye.

that KH, while providing for the reentrant effect typical of anomalous fluids, underestimates the onset of the solid phase. Summarizing, according to results presented in Figs. 13 and 14 for $\lambda = 0.2$, $\alpha = 0.8$ and $T^* = 0.0625$, the system freezes for $0.4 < \rho^* < 0.6$: on the other hand, the theoretical underestimation of the onset of the solid phase causes the density anomaly is still observed in the KH context.

IV. CONCLUSIONS

We have investigated density and structural anomalies in a dimeric fluid interacting via a purely repulsive core-softened potential by means of integral equation theories. Starting with a simple monomeric case we have progressively increased the elongation λ till to obtain a tangent configuration. We have also considered two different conditions, corresponding to one ($\alpha = 0.6$) and two ($\alpha = 0.8$) length scales of the intermolecular potential. Theoretical results have been systematically compared with already existing or newly generated Monte Carlo (MC) simulations. We have found that in the monomeric case the Ornstein-Zernike equation, coupled with hypernetted chain and Kovalenko-Hirata (KH) closures is able to accurately reproduce simulation data for internal energy and pressure if the virial equation of state is adopted. Nevertheless, the loci of density anomalies are underestimated by both the closures. Upon increasing λ we have implemented the reference interaction site model (RISM) theory coupled with KH closure; also, we have adopted a closed form for the calculation of pressure, available in the context of this closure. The theory is still able to reproduce simulation results for pressure, being less predictive for the internal energy. The fluid structure has been investigated by computing the site-site radial dis-

tribution function $g_{ij}(r)$: MC and KH agree in providing a double-peak structure for $\alpha = 0.8$, such a feature being strongly reminiscent of the double length scales of the interaction potential. This is not the case of $\alpha = 0.6$, where only a single peak in $g_{ij}(r)$ is observed. Structural and density anomalies are found for both $\alpha = 0.6$ and $\alpha = 0.8$: the theory qualitatively agrees with simulations in predicting their existence, but systematically underestimates the temperatures where they occur. In comparison with simulations, where the density anomaly is observed for $\lambda \leq 0.1$ if $\alpha = 0.6$ and for $\lambda \leq 0.3$ if $\alpha = 0.8$, KH predicts the existence of this anomaly in the whole range of elongations. This is due to the underestimation of the solid phase, that in simulations prevents the devel-

opment of this anomaly for higher values of λ . Overall, the theory proves to be reliable in providing the existence of structural and thermodynamic anomalies even if a quantitative prediction is not achieved. We emphasize that this is the first application of the RISM approach to investigate these anomalies in a fluid interacting through a core-softened potential. The possibility to have a reliable theoretical tool able to provide a quick estimate of these anomalies, whereas simulations can become more time demanding, set integral equations as promising candidates in describing fluid structure and phase behaviors of many complex fluids, such as elongated molecules, polymers and colloidal dimers.

-
- [1] Andersen H C and Chandler D 1972 *J. Chem. Phys.* **57** 1918
 - [2] Chandler D and Andersen H C 1972 *J. Chem. Phys.* **57** 1930
 - [3] Hansen J P and McDonald I R 2006 *Theory of simple liquids*, 3rd Ed. (Academic Press, New York)
 - [4] Chandler D 1978 *Ann. Rev. Phys. Chem.* **29** 441
 - [5] Lowden L J and Chandler D 1974 *J. Chem. Phys.* **61** 5228
 - [6] Johnson E and Hazoume R P 1979 *J. Chem. Phys.* **70** 1599
 - [7] Lue L and Blankschtein D 1995 *J. Chem. Phys.* **102** 5427
 - [8] Kovalenko A and Hirata F 2002 *J. Theor. Comput. Chem.* **1** 381
 - [9] Pettitt B M and Rossky P J 1983 *J. Chem. Phys.* **78** 7296
 - [10] Kvamme B 2002 *Phys. Chem. Chem. Phys.* **4** 942
 - [11] Costa D, Munaò G, Saija F and Caccamo C 2007 *J. Chem. Phys.* **127** 224501
 - [12] Hirata F 2003 *Molecular Theory of Solvation* (Kluwer Academic, Dordrecht)
 - [13] Munaò G, Costa D and Caccamo C 2009 *Chem. Phys. Lett.* **470** 240
 - [14] Munaò G, Costa D, Giacometti A, Caccamo C and Sciortino F 2013 *Phys. Chem. Chem. Phys.* **15** 20590
 - [15] Munaò G, Gámez F, Costa D, Caccamo C, Sciortino F and Giacometti A 2015 *J. Chem. Phys.* **142** 224904
 - [16] Munaò G, Costa D, Sciortino F and Caccamo C 2011 *J. Chem. Phys.* **134** 194502
 - [17] Tripathy M and Schweizer K S 2013 *J. Phys. Chem. B* **117** 373
 - [18] Kim B and Hirata F 2013 *J. Chem. Phys.* **138** 054108
 - [19] Hirata F and Akasaka K 2015 *J. Chem. Phys.* **142** 044110
 - [20] Kinoshita M and Sugay Y 2002 *J. Comput. Chem.* **23** 1445
 - [21] Kobryn A E, Nikolic D, Lyubimova O, Gusaroy S and Kovalenko A 2014 *J. Phys. Chem. B* **118** 12034
 - [22] Huang W J, Blinov N and Kovalenko A 2015 *J. Phys. Chem. B* **119** 5588
 - [23] Kung W, González-Mozuelos P and de la Cruz M O 2010 *Soft Matter* **6** 331
 - [24] Miyata T and Hirata F 2008 *J. Comput. Chem.* **29** 871
 - [25] Miyata T, Ikuta Y and Hirata F 2010 *J. Chem. Phys.* **133** 044114
 - [26] Miyata T, Ikuta Y and Hirata F 2011 *J. Chem. Phys.* **134** 044127
 - [27] Kido K, Yokogawa D and Sato H 2012 *Chem. Phys. Lett.* **531** 223
 - [28] Debenedetti P G 1996 *Metastable Liquids. Concepts and Principles* (Princeton University Press, Princeton)
 - [29] Soper A K and Ricci M A 2000 *Phys. Rev. Lett.* **84** 2881
 - [30] Dokter A M, Woutersen S and Bakker H J 2005 *Phys. Rev. Lett.* **94** 178301
 - [31] Clark G N I, Hura G L, Hura J, Soper A K and Head-Gordon T 2010 *Proc. Natl Acad. Sci. USA* **107** 14007
 - [32] Mallamace F, Corsaro C and Stanley H E 2013 *Proc. Natl. Acad. Sci. U.S.A.* **110** 4899
 - [33] Liu Y, Panagiotopoulos A Z and Debenedetti P G 2009 *J. Chem. Phys.* **131** 104508
 - [34] Sciortino F, Saika-Voivod I and Poole P H 2011 *Phys. Chem. Chem. Phys.* **13** 19759
 - [35] Kesselring T A, Franzese G, Buldyrev S V, Hermann H J and Stanley H E 2012 *Scientific Reports* **2** 474
 - [36] Poole P H, Bowles R K, Saika-Voivod I and Sciortino F 2013 *J. Chem. Phys.* **138** 034505
 - [37] Palmer J C, Martelli F, Liu Y, Car R, Panagiotopoulos A Z and Debenedetti P G 2014 *Nature* **510** 385
 - [38] Smallenburg F and Sciortino F 2015 *Phys. Rev. Lett.* **115** 015701
 - [39] Hemmer P C and Stell G 1970 *Phys. Rev. Lett.* **24** 1284
 - [40] Jagla E A 1999 *J. Chem. Phys.* **111** 8980
 - [41] Franzese G, Malescio G, Skibinsky A, Buldyrev S V and Stanley H E 2001 *Nature* **409** 692
 - [42] Skibinsky A, Buldyrev S V, Franzese G, Malescio G and Stanley H E 2004 *Phys. Rev. E* **69** 061206
 - [43] Gibson H M and Wilding N B 2006 *Phys. Rev. E* **73** 061507
 - [44] Hus M and Urbic T 2014 *Phys. Rev. E* **90** 062306
 - [45] Scala A, Sadr-Lahijany M R, Giovambattista N, Buldyrev S V and Stanley H E 2001 *Phys. Rev. E* **63** 041202
 - [46] Malescio G, Saija F and Prestipino S 2008 *J. Chem. Phys.* **129** 241101
 - [47] Buldyrev S V, Malescio G, Angell C A, Giovambattista N, Prestipino S, Saija F, Stanley H E and Xu L 2009 *J. Phys.: Condens. Matter* **21** 504106
 - [48] Gribova N V, Fomin Y D, Frenkel D and Ryzhov V N 2009 *Phys. Rev. E* **79** 051202

- [49] Prestipino S, Saija F and Malescio G 2010 *J. Chem. Phys.* **133** 144504
- [50] de Oliveira A B, Neves E B, Gavazzoni C, Paukowski J Z, Netz P A and Barbosa M C 2010 *J. Chem. Phys.* **132** 164505
- [51] Gavazzoni C, Gonzatti G K, Pereira L F, Ramos L H C, Netz P A and Barbosa M C 2014 *J. Chem. Phys.* **140** 154502
- [52] Bordin J R 2016 *Physica A* **459** 1
- [53] Kobryn A E, Yamaguchi T and Hirata F 2005 *J. Mol. Liq.* **119** 7
- [54] Huš M, Munaò G and Urbic T 2014 *J. Chem. Phys.* **141** 164505
- [55] Munaò G and Urbic T 2015 *J. Chem. Phys.* **142** 214508
- [56] Malescio G and FSaija 2011 *J. Phys. Chem. B* **115** 14091
- [57] Malescio G, Prestipino S and FSaija 2011 *Mol. Phys.* **109** 2837
- [58] Munaò G and Saija F 2016 *Phys. Chem. Chem. Phys.* **18** 9484
- [59] Kovalenko A and Hirata F 1999 *J. Chem. Phys.* **110** 10095
- [60] Kovalenko A and Hirata F 2001 *Chem. Phys. Lett.* **349** 496
- [61] Ryzhov V N and Stishov S M 2003 *Phys. Rev. E* **67** 010201(R)
- [62] Caccamo C 1996 *Phys. Rep.* **274** 1
- [63] Morita T and Hiroike K 1960 *Progr. Theor. Phys. (Japan)* **23** 1003
- [64] Singer S J and Chandler D 1985 *Mol. Phys.* **55** 621
- [65] de Oliveira A B, Netz P A, Colla T and Barbosa M C 2006 *J. Chem. Phys.* **124** 084505
- [66] Lomba E, Almaraz N G, Martin C and McBride C 2007 *J. Chem. Phys.* **126** 244510
- [67] Nettleton R E and Green M S 1958 *J. Chem. Phys.* **29** 1365
- [68] Lazaridis T and Karplus M 1996 *J. Chem. Phys.* **105** 4294
- [69] Saija F, Saitta A and Giaquinta P V 2003 *J. Chem. Phys.* **119** 3587
- [70] Esposito R, Saija F, Saitta A M and Giaquinta P V 2006 *Phys. Rev. E* **73** 040502
- [71] Huggins D J 2012 *J. Comp. Chem.* **33** 1383
- [72] Kuffel A, Czapiewski D and Zielkiewicz J 2014 *J. Chem. Phys.* **141** 055103
- [73] Munaò G, Prestipino S and Saija F *in preparation*
- [74] Truskett T M, Torquato S and Debenedetti P G 2000 *Phys. Rev. E* **62** 993
- [75] Giaquinta P V and Saija F 2005 *ChemPhysChem* **6** 1768
- [76] Cummings P T, Gray C G and Sullivan D E 1981 *J. Phys. A* **14** 1483
- [77] Hansen J P and Verlet L 1969 *Phys. Rev.* **184** 151
- [78] Giaquinta P V and Giunta G 1992 *Physica A* **187** 145
- [79] Saija F, Prestipino S and Giaquinta P V 2006 *J. Chem. Phys.* **124** 244504